Evaluation of Matrix Metalloproteinases in Atherosclerosis Using a Novel Noninvasive Imaging Approach

Eric Lancelot*, Vardan Amirbekian*, Irène Brigger*, Jean-Sébastien Raynaud, Sébastien Ballet, Christelle David, Olivier Rousseaux, Soizic Le Greneur, Marc Port, Henri R. Lijnen, Patrick Bruneval, Jean-Baptiste Michel, Tanja Ouimet, Bernard Roques, Smbat Amirbekian, Fabien Hyafil, Esad Vucic, Juan Gilberto S. Aguinaldo, Claire Corot, Zahi A. Fayad

Objective—Despite great advances in our knowledge, atherosclerosis continues to kill more people than any other disease in the Western world. This is because our means of identifying truly vulnerable patients is limited. Prediction of atherosclerotic plaque rupture may be addressed by MRI of activated matrix metalloproteinases (MMPs), a family of enzymes that have been implicated in the vulnerability of plaques prone to rupture. This study evaluated the ability of the novel gadolinium-based MRI contrast agent P947 to target MMPs in atherosclerotic plaques.

Methods and Results—The affinity of P947 toward activated MMPs was demonstrated in vitro. The affinity and specificity of P947 toward matrix metalloproteinase (MMP)-rich plaques was evaluated both in vivo using ApoE$^{-/-}$ mice and ex vivo in hyperlipidemic rabbits. Gadolinium content quantification and MRI showed a preferential accumulation of P947 in atherosclerotic lesions compared with the nontargeted reference compound, Gd-DOTA. The ex vivo assay on rabbit plaques revealed a higher uptake of P947. Moreover, using human carotid artery endarterectomy specimens, P947 facilitated discrimination between histologically defined MMP-rich and MMP-poor plaques. An in vivo MRI investigation in mice revealed that P947 greatly improved the ability to visualize and delineate atherosclerotic plaques.

Conclusions—P947 may be a useful tool for the detection and characterization of the MMP-rich atherosclerotic plaques. (***Arterioscler Thromb Vasc Biol*. 2008;28:425-432**)

Key Words: atherosclerosis ■ matrix metalloproteinases ■ MRI ■ atherosclerotic plaque ■ molecular imaging

Molecular imaging is a promising modality for assessment of atherosclerotic plaque composition.[1] It may enable the detection of biological markers whose expression is directly related to the pathophysiological status of the lesions.[2,3] Recently, MRI has been used to assess activated plaques by detecting human macrophages with ultra-small superparamagnetic particles of iron oxide (Sinerem®),[4] rabbit angiogenesis with AlphaVbeta3 targeting nanoparticles,[5] rabbit thrombosis with a fibrin-binding contrast agent (EP-1873),[6] and murine macrophages with scavenger receptor-targeted immunomicelles.[7] Finally, apoptotic plaque macrophages were visualized with [^{99m}Tc]-labeled annexin V in carotid arteries of symptomatic patients.[8]

By applying high-resolution multi-contrast in vivo MRI, some features of vulnerability, such as cap rupture, large necrotic core, or intraplaque hemorrhage, have become detectable in human carotid arteries.[9] Molecular imaging may substantially improve the accuracy of MRI detection by selectively revealing specific markers of instability. One such marker is represented by matrix metalloproteinases (MMPs), which are overexpressed in prone-to-rupture atherosclerotic lesions as a consequence of inflammation.[10] MMPs promote plaque destabilization by degrading the fibrillar collagen of the fibrous cap and are overexpressed in the shoulder regions of human atherosclerotic plaques, the most common site of rupture.[11] Recent work has demonstrated that experimental overexpression of MMPs led to cardinal features of plaque rupture in a mouse model of atherosclerosis.[12] Therefore, MMP expression is not only a part of atherosclerosis pathogenesis but may also be predictive of plaque instability.[13,14]

The aim of the present study was to evaluate the ability of the MRI contrast agent P947 to target activated MMPs in atherosclerotic plaques. The affinity of P947 was first tested in vitro on purified MMPs. The biodistribution was studied in

Original received March 21, 2007; final version accepted December 10, 2007.

From the Imaging Science Laboratories, Department of Radiology, the Zena and Michael A. Wiener Cardiovascular Institute, the Marie-Josée and Henry R. Kravis Cardiovascular Health Center, and Department of Medicine, Mount Sinai School of Medicine (V.A., S.A., F.H., E.V., J.G.S.A., Z.A.F); Guerbet (E.L., I.B., J-S.R., S.B., C.D., O.R., S.LG., M.P., C.C.), Aulnay-sous-Bois, France; Center for Molecular and Vascular Biology (H.R.L.), University of Leuven, Belgium; INSERM U-652 (P.B.), Paris, France; INSERM U-698 (J-B.M.), Paris, France; Pharmaleads (T.O., B.R.), Paris, France; Emory University School of Medicine (S.A.), Atlanta, Ga; Brigham and Women's Hospital (V.A.), Harvard Medical School, Boston, Mass; and the Sarnoff Cardiovascular Research Foundation (V.A.).

*E.L., V.A., and I.B. contributed equally to this study.

Correspondence to Zahi A. Fayad, PhD, FAHA, FACC, Translational and Molecular Imaging Institute, Mount Sinai School of Medicine, Box 1234, One Gustave L. Levy Place, New York, NY 10029. E-mail Zahi.Fayad@mssm.edu

Arterioscler Thromb Vasc Biol **is available at http://atvb.ahajournals.org** **DOI: 10.1161/ATVBAHA.107.149666**

the apolipoprotein E knockout ($ApoE^{-/-}$) mouse model of atherosclerosis to demonstrate its preferential accumulation in plaques. Ex vivo MRI was carried out on hyperlipidemic rabbit lesions to investigate the mechanisms of its interaction with the tissue MMPs. Ex vivo MRI was also performed on human carotid endarterectomy specimens to appreciate the capacity of P947 to differentiate MMP-rich and MMP-poor plaques. Finally, to demonstrate the in vivo feasibility of active MMP detection by MRI, an in vivo MRI investigation was performed in the $ApoE^{-/-}$ mouse model of atherosclerosis. Various types of in vivo controls were used to validate the results.

Methods

Contrast Agents and In Vitro Binding Assay

P947 was obtained by coupling an MMP inhibitor to the gadolinium (Gd) chelate, 1,4,7,10-tetraazacyclododecane-N, N′, N′′, N′′′-tetraacetic acid (DOTA). See the Methods supplement for details. P947 has a molecular weight of 1210 Da and an r1 relaxivity value of 5.5 $mmol/L^{-1}$ s^{-1} in water at 1.5 T and 37°C. Gd-DOTA, a standard nonspecific gadolinium contrast agent with an r1 relaxivity value of 3.7 $mmol/L^{-1}$ s^{-1}, was used as the reference compound. The affinities of P947, the free peptide and Gd-DOTA toward MMPs were studied in vitro on human purified MMP-1, -2, -3, -8, -9, -13, and -14. The assay was based on the detection of a fluorescent product resulting from the MMP-induced cleavage of a specific substrate. See the Methods supplement (available online at http://atvb.ahajournals.org) for details.

In Vivo Distribution Assay

Atherosclerotic $ApoE^{-/-}$ mice (C57BL/6) were injected with P947 or Gd-DOTA (100 μmol/kg, IV) via the tail vein. One hour later a blood sample was collected via infraorbital puncture. Muscle, kidney, liver, carotid arteries, aortic arch, thoracic aorta, abdominal aorta, and femoral arteries were collected. The concentrations of the contrast agents were determined by quantifying Gd using inductively coupled plasma–mass spectrometry (ICP-MS). In situ zymography was performed on frozen sections proximal to the aortic valves of either $ApoE^{-/-}$ mice injected with P947 or $ApoE^{-/-}$ mice that were not injected at all. See the Methods supplement for details.

Ex Vivo MRI Assay

The thoracic aortas were collected from atherosclerotic Watanabe Heritable Hyperlipidemic (WHHL) rabbits and then incubated with the contrast agents and used for ex vivo MR imaging. Fresh human carotid artery specimens were collected from 21 atherosclerotic patients undergoing carotid endarterectomy. The stenosing complicated zone, at the origin of the internal carotid artery, was dissected and separated from the adjacent plaque, at the common and external carotid arteries. See the Methods supplement for details. Rabbit or fresh human specimens were incubated with either P947 or Gd-DOTA (0.5 mmol/L final concentration). For specificity testing, some rabbit samples were incubated for 18 hours with P947 (0.5 mmol/L) in the presence of an excess concentration of free peptide (5.0 mmol/L). The human and rabbit samples were submitted to 18 hours of incubation, followed by washing with Krebs-Ringer bicarbonate buffer. Ex vivo MRI was performed on the samples. See the Methods supplement for details. After ex vivo imaging, the samples were submitted to acidic mineralization and Gd quantification by ICP-MS. Immunohistochemical analyses were performed on cryostat sections of human internal carotid plaques to demonstrate the presence of α-actin, CD68 macrophage marker, MMP-1, -2, -3, -7, -9. See the Methods supplement for details.

Ex Vivo Affinity Assay

To demonstrate the interaction between P947 and MMPs in atherosclerotic tissues, another set of experiments was performed on human carotid plaques. A second series of fresh samples was collected from 14 patients after carotid endarterectomy. These samples were incubated in culture medium. After 24 hours, the conditioned culture media were collected for use. A MMP enzymatic activity assay was designed to quantify the MMP activity present in the conditioned culture media using a fluorescently quenched peptide that is cleaved, releasing fluorescence, by MMP-1, -2, -7, -8, -9, -12, -13, -14, -15, and -16. See the Methods supplement for details. Released fluorescence, representing total activity, was measured at λex=340 nm and λem=405 nm on a Twinkle LB970 apparatus (Berthold, Germany). Nonspecific enzymatic activity was measured in the same conditions except for the addition of the metal chelating agent EDTA (1 mmol/L), which is a potent MMP inhibitor. To evaluate the inhibitory potency (IC_{50} values) of P947 on the ensemble of the MMPs expressed by the excised carotid tissues, the compound was incubated in increasing concentrations ranging from 10 nmol/L to 1 μmol/L. The value obtained in the presence of 1 mmol/L EDTA was subtracted from each point to obtain a specific MMP activity.

In Vivo MRI Assay

After a preinjection baseline MRI scan, $ApoE^{-/-}$ mice (n=8) were injected P947 (100 μmol/kg, IV) via the tail vein. For controls, $ApoE^{-/-}$ mice (n=4) were injected the standard gadolinium contrast agent Gd-DOTA (100 μmol/kg, IV). As additional controls, WT mice were injected with equivalent doses of P947 (100 μmol/kg, IV). After injection, postcontrast MRI was performed at 1, 2, 3, and 22 hours. See the Methods supplement for details. Slices were precisely anatomically matched to the slices obtained on the preinjection baseline scan. The pathological slides of the atherosclerotic aortas, from mice used in the experiments, were matched to the MRI slices for comparison and correlation. For each matched slice the Normalized Enhancement Ratio (NER) was used to calculate the enhancement of the aortic wall post-contrast injection using Equation 1:

(1)

$$NER = \frac{\left(\frac{(W_{1POST}+W_{2POST}+W_{3POST}+W_{4POST})}{4}\right) \Big/ \text{SI of Muscle Post-Contrast}}{\left(\frac{(W_{1PRE}+W_{2PRE}+W_{3PRE}+W_{4PRE})}{4}\right) \Big/ \text{SI of Muscle Pre-Contrast}}$$

Where W_{nPOST} is the SI of the aortic wall in quadrant n, after injection of contrast agent. W_{nPRE} is the SI of the aortic wall in quadrant n, before injection of contrast agent.

Statistical Analysis

The Gd concentrations were compared with the unpaired, nonparametric, Mann–Whitney test, using a 2-tailed probability value. The MMP activities of the internal carotid artery and of the common or external carotid arteries were compared with a paired Student *t* test. The NER data were compared between different time points using a paired *t* test with adjacent time points as reference. Differences were considered significant at $P<0.05$. See the Methods supplement for further details.

Results

In Vitro Binding Assay

Contrary to Gd-DOTA, P947 inhibited the activity of the seven tested MMPs (supplemental Table I). Its affinity is in the micromolar range for the soluble MMP-1, -2, -3, -8, -9, and -13 and about 100 times lower for the membrane-type MMP-14. The IC_{50} values of P947 are consistent with those of the free peptide which were both obtained experimentally for MMP-1, -2, -3, -8, -9, and -13, and reported by Odake et al for MMP-1, -3, -8, and -9.[15]

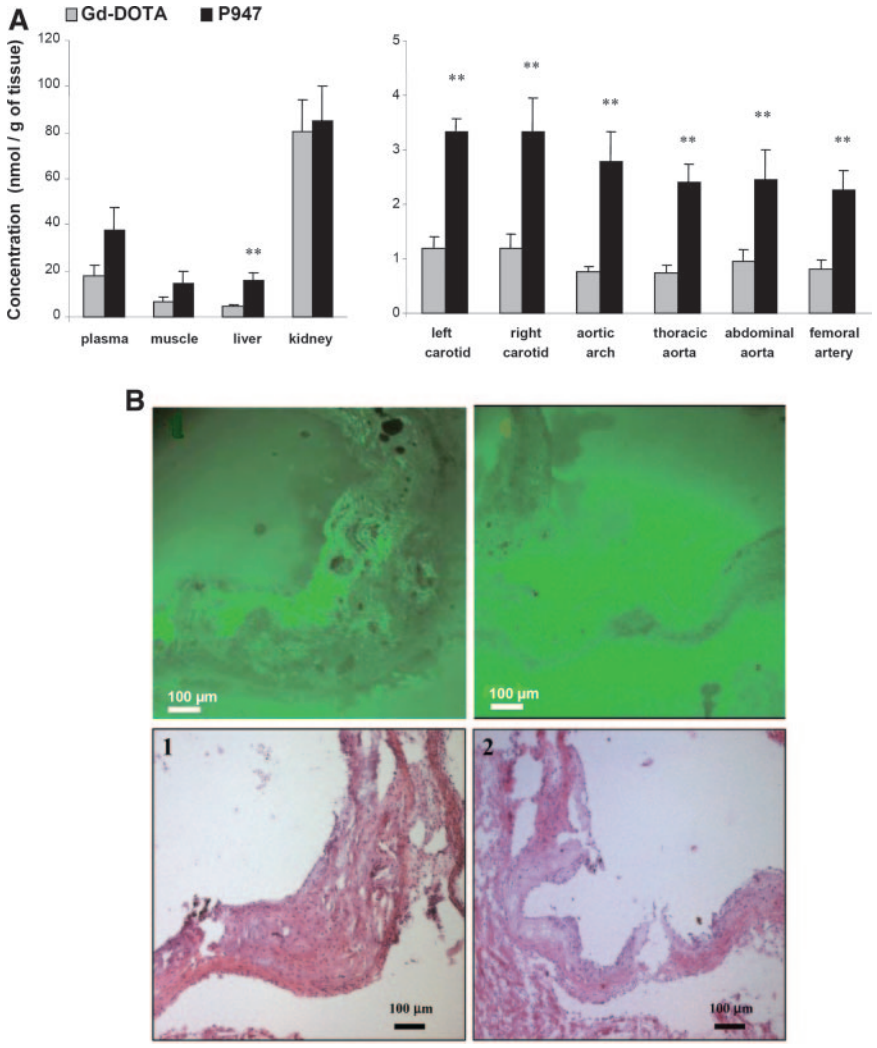

Figure 1. A) Biodistribution of P947 and Gd-DOTA. B) Top Row, In situ gelatin zymography of atherosclerosis. Left column, Saline-treated control sections from ApoE$^{-/-}$ mice. Right column, P947-treated sections. Dark spots represent areas of MMP lysis/activity. Bottom, Corresponding hematoxylin/eosin stained sections of the same areas as the top row.

In Vivo Distribution Assay

One hour after intravenous injection into ApoE$^{-/-}$ mice, no significant differences were observed in plasma, kidney, and muscle concentrations between P947 and Gd-DOTA, whereas the liver uptake was increased 3-fold for P947 (Figure 1A). The compounds had a plasma half-life of 30 and 15 minutes, respectively. They were rapidly cleared from the body as the residual fractions still present in the plasma and the main organs after 1 hour amounted to only 2% to 4% of the injected dose. Their concentrations were highest in the kidney.

P947 concentrations in the artery specimens were approximately 3 times as high as those of Gd-DOTA ($P<0.01$; Figure 1A). However, there was no significant difference between the arterial wall segments.

In this model, extensive atherosclerotic lesions developed on the aortic valves and arch (data not shown). Atherosclerotic heart sections from ApoE$^{-/-}$ mice were used to visualize active MMPs by in situ zymography. There was a lower density of dark spots in the sections from P947-treated animals than from the control mice (Figure 1B), which suggests that MMPs were less able to induce lysis of the substrate gel.

Ex Vivo Assays

Immediately after the incubation phase, P947 produced a stronger signal enhancement of the rabbit arterial wall than Gd-DOTA (Figure 2A). The latter compound tended to diffuse rapidly in the surrounding gel. Moreover, after the washing phase, Gd-DOTA was totally cleared from the samples whereas P947 remained bound to the tissues, even after prolonged periods of elution. These ex vivo MRI findings were confirmed by the Gd measurements that showed a persistent accumulation of P947 in the tissues ($P<0.001$ versus Gd-DOTA, Figure 2B). The binding of P947 was competitively inhibited when the free peptide was applied in excess concentration ($P<0.001$ versus without free peptide, Figure 2C and 2D).

By immunohistochemical analysis, we show that various types of MMPs (MMP-1, -2, -3, -7, and -9) were present in the human plaques of the internal carotid artery. MMP-3 displayed relatively more intense staining, whereas MMP-2 was more diffuse and less detectable (supplemental Figure I). These MMP-rich plaques also contained α-actin positive smooth muscle cells in the media and CD68 positive macrophages at the shoulders and at the interface between the core and the fibrous cap (supplemental Figure I). Calcifications were also common.

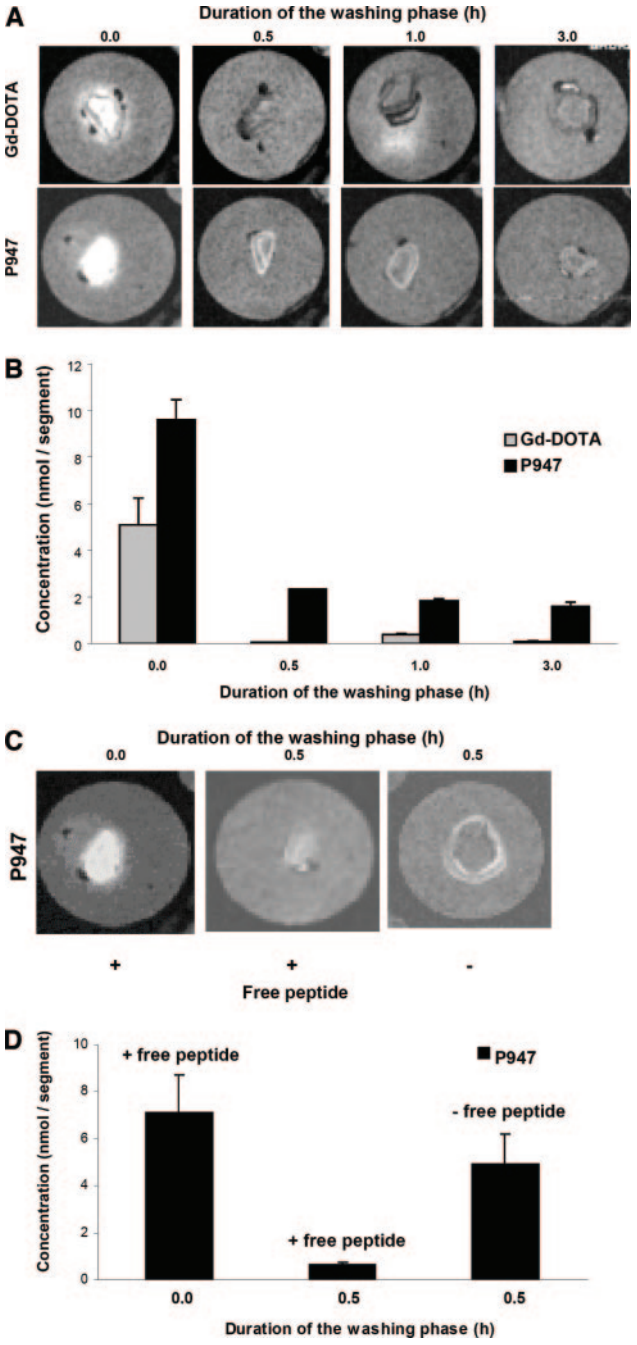

Figure 2. A, Ex vivo MRI of WHHL rabbit aortas showing a higher retention of P947 than Gd-DOTA. B, Corresponding P947 and Gd-DOTA concentrations in WHHL rabbit samples. C, Ex vivo MRI of WHHL rabbit aortas demonstrating competitive inhibition of P947 binding by the free peptide. D, Corresponding P947 concentrations in WHHL rabbit samples.

Although they may have specific substrates, many MMPs are also able to cleave the same molecules. Such a common substrate, when applied on conditioned media obtained after incubation of human atherosclerotic plaques, allows for the global quantification of the MMP activity expressed in the samples. This quantification was performed on a set of carotid artery specimens collected from 14 atherosclerotic patients undergoing carotid endarterectomy. The results obtained showed a significant difference in the MMP activity expressed in conditioned media from atherosclerotic plaques of the internal carotid artery (618±158 AU/mg of tissue) compared with the common and external carotid arteries (125±21 AU/mg of tissue, $P<0.01$). Thus, MMP-rich lesions of the internal carotid artery expressed approximately 5 times more specific MMP activity than MMP-poor lesions of the common and external carotid arteries. Both MMP-rich and MMP-poor carotid artery specimens, collected from 21 atherosclerotic patients, were incubated with P947 or Gd-DOTA and imaged by MRI. P947 and, to a lesser extent, Gd-DOTA showed a marked enhancement of signal in the segments when ex vivo MRI was performed immediately after the incubation period (Figure 3A, left). However, after the washing phase, Gd-DOTA could no longer be detected, whereas P947 was still present and visible. Only P947 allowed differentiation between MMP-rich and MMP-poor atherosclerotic lesions. These MRI observations were corroborated by the Gd concentration measurements showing that both types of lesions accumulated 10 times more P947 than Gd-DOTA (Figure 3B). Moreover, P947 concentration was significantly higher in the MMP-rich than in the MMP-poor plaques (59±6 versus 38±3 nmolGd/g of tissue, corresponding to 7.3% versus 3.4% of the amount added to the incubation medium, $P<0.01$). Such a difference could not be observed with Gd-DOTA ($P=0.27$).

To further support the hypothesis that P947 targets MMPs in vivo, the ex vivo binding characteristics of the compound was investigated. These results provide IC_{50} values for P947, which are in agreement with the values obtained in vitro against individual MMPs that are mostly in the micromolar range. Indeed, P947 inhibited global MMP activity in conditioned media with affinities ranging from 5 to 12 μmol/L for both MMP-rich and MMP-poor plaques (Figure 4). Moreover, the mean IC_{50} value obtained from conditioned media from MMP-rich plaques (8.6±3.0 μmol/L) was not different from that of MMP-poor plaques (7.5±2.8 μmol/L). Taken together, these results suggest that P947 efficiently inhibits MMP activities in atherosclerotic plaques ex vivo, thus demonstrating an active targeting.

In Vivo MRI Assay

In the ApoE$^{-/-}$ mice that were injected with P947, excellent delineation of plaque, with strong SI enhancement, was seen in the atherosclerotic aortas using MRI. The pattern of enhancement was heterogeneous in nature, consistent with known patterns of atherosclerotic plaque distribution in the aortas of ApoE$^{-/-}$ mice. The MRI results correlated well with the matched pathology findings (Figure 5). There was a statistically significant increase in the CNR (Equation 1) on post-contrast-enhanced images at 1, 2, and 3 hours postinjection of P947. Using P947 in ApoE$^{-/-}$ mice, the average CNR increased to 17.10±1.59 at 1 hour postinjection compared with 7.57±1.61 at the preinjection baseline ($P<0.0001$). At 2, 3, and 22 hours postinjection, the average CNRs were 10.90±1.35 ($P<0.0001$ versus preinjection), 9.86±1.93 (P=NS), and 7.49±1.81 (P=NS), respectively. Conversely, in ApoE$^{-/-}$ mice that were injected with the standard contrast agent Gd-DOTA, the CNR of the aortic wall changed to 4.71±1.68 at 1 hour after injection compared with a baseline

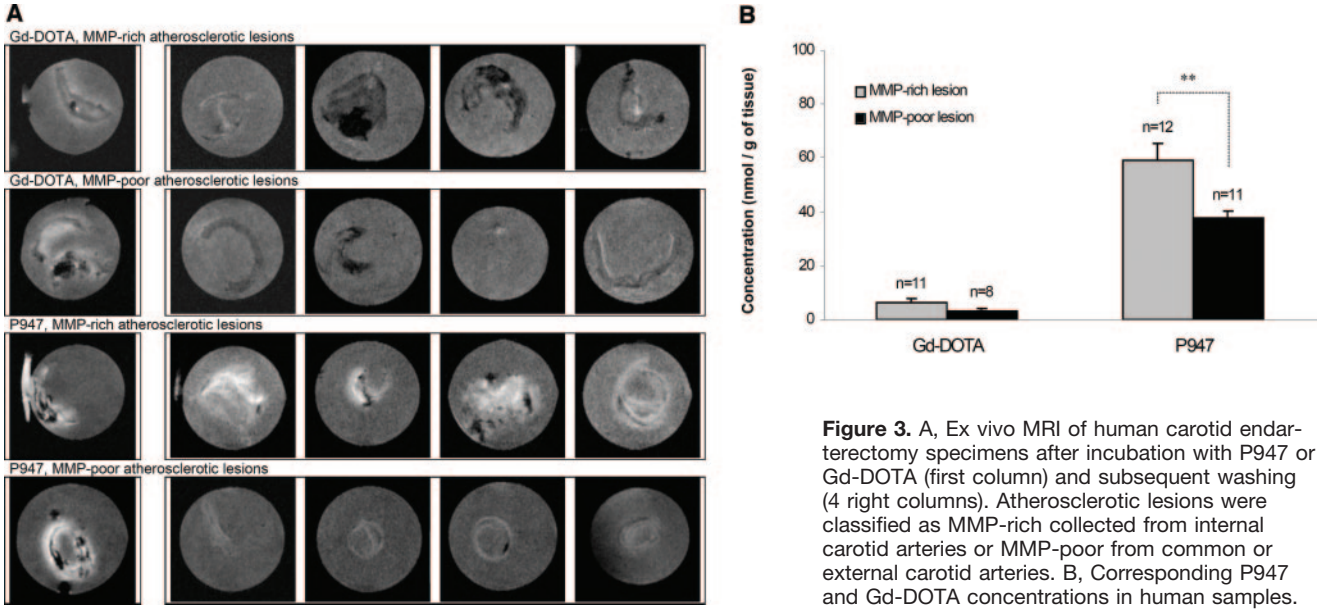

Figure 3. A, Ex vivo MRI of human carotid endarterectomy specimens after incubation with P947 or Gd-DOTA (first column) and subsequent washing (4 right columns). Atherosclerotic lesions were classified as MMP-rich collected from internal carotid arteries or MMP-poor from common or external carotid arteries. B, Corresponding P947 and Gd-DOTA concentrations in human samples.

value of 8.11±2.67 ($P<0.05$). The changes in CNR using Gd-DOTA were not statistically significant at any other time points scanned.

The NER (from Equation 1) representing the post- to the precontrast SI of the aortic wall, normalized to muscle, with P947 was an average of 1.95±0.17 (95% normalized SI enhancement; $P<0.0001$ compared with the 22-hour time point) in the ApoE$^{-/-}$ mice at 1 hour, 1.51±0.13 (51% normalized SI enhancement; $P<0.0001$ compared with the 22-hour time point) at 2 hours, 1.19±0.12 (19%) at 3 hours, and 1.09±0.09 (9%) at 22 hours (Figure 6). In the control ApoE$^{-/-}$ mice that were injected with the standard agent Gd-DOTA, there was minimal homogeneous SI enhancement of the aortic wall with no statistically significant increase of the NER. In the WT mice that were injected with P947, there was no statistically significant enhancement using the NER and minimal changes in the CNR. Finally, Gd-DOTA produced no significant SI enhancement in WT mice (data not shown).

Discussion

The primary aim of our study was to evaluate whether P947 has the potential to facilitate atherosclerotic plaque detection using targeted MRI of MMPs. The in vitro assay on purified MMPs showed that the free peptide, which is the targeting constituent of P947, is a broad spectrum MMP inhibitor that binds active enzymes at micromolar concentrations. The affinities of P947 toward MMPs were not significantly different from those of the parent compound, demonstrating that coupling of the contrast moiety did not alter the properties of the peptide.

The in vivo biodistribution assay in ApoE$^{-/-}$ mice showed that the pharmacokinetic profile of P947 was similar to that of Gd-DOTA. Despite the similar clearance, P947 accumulated approximately 3 times more than Gd-DOTA in most artery walls. In the carotid arteries and aortic arch, which contain large atherosclerotic plaques with high levels of MMPs, P947 concentrations were in the micromolar range. The fact that these concentrations are higher than those of the reference compound, and consistent with the IC_{50} values for MMPs, is in favor of specific binding of P947 to MMPs in the lesions. This hypothesis is further supported by the in situ zymography assay showing that the gelatinolytic activity of atherosclerotic plaques was decreased when the ApoE$^{-/-}$ mice were pretreated with P947. Further work is planned in future investigations to provide additional evidence of specific binding.

The ex vivo assay on rabbit aortic rings was set up to study, by MRI and by Gd concentration measurement, the mechanisms of interaction between P947 and MMPs in a model independent of any pharmacokinetic or anatomic consideration. In comparison to Gd-DOTA, over time P947 showed higher uptake in and lower elution from atherosclerotic plaques of WHHL rabbits. This retention, as well as the efficacy of the competition when the free peptide was added in excess to the incubation medium, indicates that P947 binds to a component of plaques. As immunohistochemical analyses confirmed the presence of MMPs in the specimens, it is likely that P947 accumulated in the plaques because of its efficient binding to MMPs.

The ex vivo assays on human carotid endarterectomy specimens were designed to evaluate whether P947 could be helpful for the characterization of atherosclerotic plaques. First, immunohistochemical analyses revealed the presence of MMP-1, -2, -3, -7, and -9 in the complicated lesions of the internal carotid artery, which is consistent with the literature.[16,17] Second, we showed that these plaques express statistically significantly greater MMP activity when compared with those of the common or external carotid arteries, which is in favor of a more vulnerable phenotype, as previously reported.[17–19] Both MR images and Gd measurements demonstrated a higher accumulation of ex vivo–applied P947 in the MMP-rich lesions of the internal carotid artery than in the MMP-poor ones of the common and external carotid arteries, whereas Gd-DOTA did not show any particular affinity for the tissues. The concentration of P947 in the MMP-rich plaques was again in the micromolar

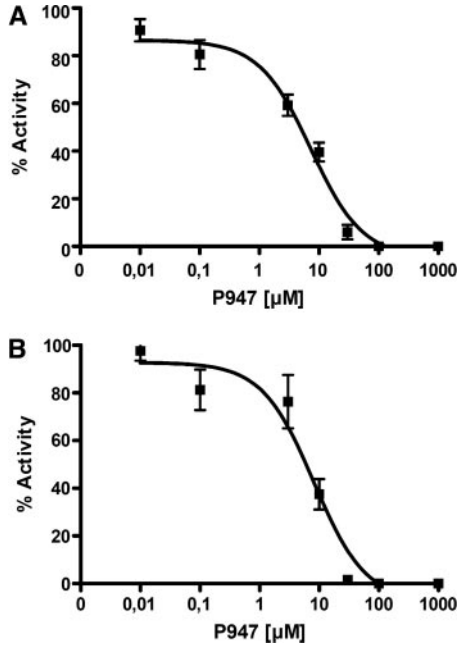

Figure 4. Increasing concentrations of P947 were placed in the presence of conditioned media from 3 different MMP-rich (A) or MMP-poor (B) plaques. The mean IC_{50} values of 3 plotted experiments are of 8.6±3.0 μmol/L and 7.5±2.8 μmol/L (±SD) for the MMP-rich and MMP-poor plaques, respectively.

range. These data demonstrate that P947 accumulates in human plaques at a concentration that is compatible with MR detection and suggest that it may have the capacity to identify vulnerable plaques. Subsequently, to further support the hypothesis that this accumulation is specifically related to MMPs, we studied the binding characteristics of P947 on MMP-rich and MMP-poor plaque medium derivatives. P947 displayed an MMP inhibitory activity with IC_{50} values in the micromolar range for both types of plaques. This indicates that there is no difference between the affinities of P947 for

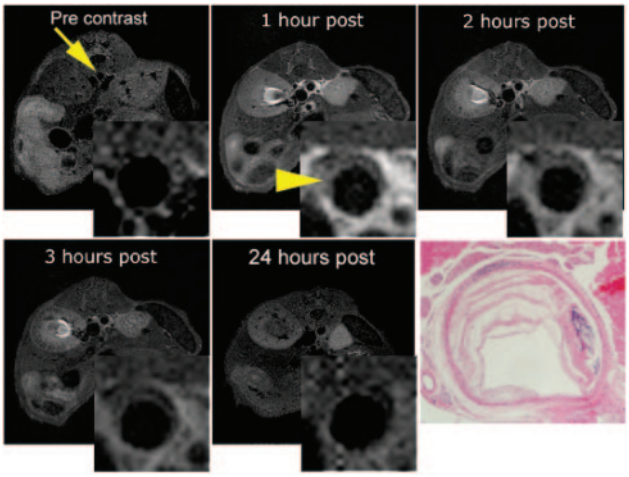

Figure 5. In vivo MRI of an ApoE$^{-/-}$ mouse before (arrow) and after P947 injection (arrowhead). After injection, significant contrast-enhancement appears in the atherosclerotic aortic wall as shown on the inset images of the aorta. Delineation of plaque morphology after contrast-enhancement is clearly improved (arrowhead). The bottom-right panel is the matched pathologic section.

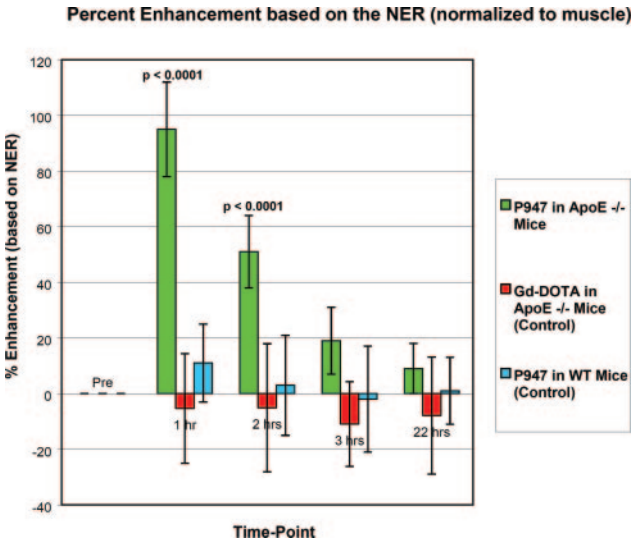

Figure 6. The graph shows the change in MRI signal intensity of the aorta that was observed in the different groups of mice. The graph bars show percent enhancement of NER (±SD) in ApoE$^{-/-}$ mice that were injected with P947 (green), Gd-DOTA (red), and in wild-type mice injected with P947 (blue).

MMPs in vulnerable versus more stable plaques. Thus, the observed difference in P947-mediated MR enhancement of MMP-rich versus MMP-poor plaques is primarily a function of the higher concentration of active MMPs in the former than in the latter. Overall, these data provide additional evidence for the hypothesis that P947 specifically binds MMPs in atherosclerotic plaques.

The in vivo MRI investigations of P947 in ApoE$^{-/-}$ mice were quite promising. The MMP-targeting compound clearly delineated plaques better than Gd-DOTA or when imaging without a contrast agent. Interestingly, as a general visual observation, the pattern of enhancement seen on images demonstrated higher signal intensities at the fibrous cap, the shoulder regions of plaques and the outer layers of plaques. Conversely, there was little enhancement seen in the lipid-rich core regions of plaques. These observations are consistent with studies of MMP expression in atherosclerotic plaques.[20] Interestingly, the previously published patterns of MMP immunostaining on sections of plaques are strikingly similar to the patterns of SI enhancement seen on MRI in our studies using P947.[11,21,22] Overall, the in vivo results in mice are encouraging and suggest that experiments in a larger model of atherosclerosis, such as a rabbit model, are warranted.

A growing body of evidence has implicated MMPs in the remodeling and destabilization of atherosclerotic plaques.[16,17,23,24] Our immunohistological observations confirm these data showing a heterogeneous and diffuse distribution of the main MMPs in the necrotic core of the carotid culprit plaques. MMP-1 expression was reported to be twice as great in the regions with highest circumferential tensile stress, in the fibrous cap of human coronary lesions.[25] MMP-1, -8, and -13 expressions were found to be 3 times higher in atheromatous than in fibrous carotid plaques.[18,26] MMP-9 was observed more frequently in coronary lesions of patients with unstable rather than stable angina.[27] The concentration of MMP-9 was

increased 4-fold in unstable plaques of symptomatic patients undergoing carotid endarterectomy compared with asymptomatic ones.[19] Recently, experimentally designed overexpression of MMP-9 led to the development of vulnerable rupture-prone plaques in ApoE$^{-/-}$ mice.[12] Altogether, these data suggest that vulnerable plaques, which contain a higher density of activated macrophages and intraplaque hemorrhages at different stages,[28,29] are characterized by higher levels of MMPs. Some of these MMPs may precipitate the rupture of the fibrous cap by specifically weakening the extracellular matrix in regions subjected to increased mechanical stresses. MMPs therefore represent a promising target, both for therapy and for molecular imaging.

The nonselective MMP inhibitors, batimastat and marimastat, efficiently prevented restenosis after balloon dilatation in atherosclerotic pigs.[30] However, they did not induce any reduction of plaque burden in LDLR-KO mice.[31] Recently, scintigraphic imaging was performed with the broad spectrum MMP inhibitor [^{123}I]-CGS 27023A.[20] It allowed the in vivo detection of MMP-rich vascular lesions in ApoE$^{-/-}$ mice. MRI has many advantages compared with scintigraphic imaging methods, which suffer from low anatomic resolution, or to optical imaging techniques, which are not suitable for noninvasive investigations of the deep tissue layers. However, the success of molecular MR imaging approaches depends directly on the concentration and accessibility of the molecular targets and on the MR efficacy of the contrast agents. In the context of MMPs, the targets are present in the extracellular matrix and can therefore easily be reached by P947. Concerning their concentration, we calculated from data in the literature that the content of MMPs is at least 50 nmol/L in advanced human plaques. Even though this value is underestimated, because the information was not available for all MMP subtypes, MMP concentrations are on the low side. It appears therefore mandatory to target a majority of MMP subtypes to yield sufficient signal intensity. The originality of P947 is that its targeting moiety is optimal for molecular MRI thanks to a broad spectrum MMP inhibition and an affinity in the micromolar range.

Characterization of plaque composition represents a new goal for noninvasive identification of vulnerable lesions and many cellular/molecular imaging agents are currently being evaluated.[2,3] We provided evidence that P947 has a good affinity for purified MMPs and that it accumulates in vivo in atherosclerotic lesions of ApoE$^{-/-}$ mice. We demonstrated ex vivo that P947 binds preferentially to human MMP-rich carotid plaques. Additionally, we showed the efficacy of P947 for in vivo detection of atherosclerotic plaques using high-resolution MRI in the ApoE$^{-/-}$ mouse model of atherosclerosis. Overall, these data suggest that P947 may become a useful imaging tool for noninvasive detection of MMP activity in the evaluation of atherosclerosis.

Acknowledgments

The authors thank Christine Laclédère, Liliane Louedec, Sou-Vinh Orng, and Xavier Violas for their excellent technical assistance in this work.

Sources of Funding

Partial support was provided by NIH/NHLBI RO1 HL71021, NIH/NHLBI HL78667 (ZAF), the Zena and Michael A. Wiener Cardiovascular Institute, the Marie-Josée and Henry R. Kravis Cardiovascular Health Center, the Department of Radiology, Mount Sinai School of Medicine, Guerbet, France, the Fédération Française de Cardiologie (to F.H.), and the Sarnoff Cardiovascular Research Foundation (to V.A.).

Disclosures

None.

References

1. Choudhury RP, Fuster V, Fayad ZA. Molecular, cellular and functional imaging of atherothrombosis. *Nat Rev Drug Discov*. 2004;3:913–925.
2. Lipinski MJ, Fuster V, Fisher EA, Fayad ZA. Technology insight: targeting of biological molecules for evaluation of high-risk atherosclerotic plaques with magnetic resonance imaging. *Nat Clin Pract Cardiovasc Med*. 2004;1:48–55.
3. Fayad ZA, Amirbekian V, Toussaint JF, Fuster V. Identification of interleukin-2 for imaging atherosclerotic inflammation. *Eur J Nucl Med Mol Imaging*. 2006;33:111–116.
4. Kooi ME, Cappendijk VC, Cleutjens KB, Kessels AG, Kitslaar PJ, Borgers M, Frederik PM, Daemen MJ, van Engelshoven JM. Accumulation of ultrasmall superparamagnetic particles of iron oxide in human atherosclerotic plaques can be detected by in vivo magnetic resonance imaging. *Circulation*. 2003;107:2453–2458.
5. Winter PM, Morawski AM, Caruthers SD, Fuhrhop RW, Zhang H, Williams TA, Allen JS, Lacy EK, Robertson JD, Lanza GM, Wickline SA. Molecular imaging of angiogenesis in early-stage atherosclerosis with alpha(v) beta3-integrin-targeted nanoparticles. *Circulation.* 2003; 108:2270–2274.
6. Sirol M, Fuster V, Badimon JJ, Fallon JT, Moreno PR, Toussaint JF, Fayad ZA. Chronic thrombus detection with in vivo magnetic resonance imaging and a fibrin-targeted contrast agent. *Circulation*. 2005;112: 1594–1600.
7. Amirbekian V, Lipinski MJ, Briley-Saebo KC, Amirbekian S, Aguinaldo JG, Weinreb DB, Vucic E, Frias JC, Hyafil F, Mani V, Fisher EA, Fayad ZA. Detecting and assessing macrophages in vivo to evaluate atherosclerosis noninvasively using molecular MRI. *Proc Natl Acad Sci U S A*. 2007.
8. Kietselaer BL, Reutelingsperger CP, Heidendal GA, Daemen MJ, Mess WH, Hofstra L, Narula J. Noninvasive detection of plaque instability with use of radiolabeled annexin A5 in patients with carotid-artery atherosclerosis. *N Engl J Med*. 2004;350:1472–1473.
9. Cai JM, Hatsukami TS, Ferguson MS, Small R, Polissar NL, Yuan C. Classification of human carotid atherosclerotic lesions with in vivo multicontrast magnetic resonance imaging. *Circulation*. 2002;106: 1368–1373.
10. Loftus IM, Naylor AR, Bell PR, Thompson MM. Matrix metalloproteinases and atherosclerotic plaque instability. *Br J Surg*. 2002;89: 680–694.
11. Galis ZS, Sukhova GK, Lark MW, Libby P. Increased expression of matrix metalloproteinases and matrix degrading activity in vulnerable regions of human atherosclerotic plaques. *J Clin Invest*. 1994;94: 2493–2503.
12. Gough PJ, Gomez IG, Wille PT, Raines EW. Macrophage expression of active MMP-9 induces acute plaque disruption in apoE-deficient mice. *J Clin Invest*. 2006;116:59–69.
13. Galis ZS. Vulnerable plaque: the devil is in the details. *Circulation*. 2004;110:244–246.
14. Khatri JJ, Johnson C, Magid R, Lessner SM, Laude KM, Dikalov SI, Harrison DG, Sung HJ, Rong Y, Galis ZS. Vascular oxidant stress enhances progression and angiogenesis of experimental atheroma. *Circulation*. 2004; 109:520–525.
15. Odake S, Morita Y, Morikawa T, Yoshida N, Hori H, Nagai Y. Inhibition of matrix metalloproteinases by peptidyl hydroxamic acids. *Biochem Biophys Res Commun*. 1994;199:1442–1446.
16. Leclercq A, Houard X, Loyau S, Philippe M, Sebbag U, Meilhac O, Michel JB. Topology of protease activities reflects atherothrombotic plaque complexity. *Atherosclerosis.* 2007;191:1–10.
17. Choudhary S, Higgins CL, Chen IY, Reardon M, Lawrie G, Vick GW 3rd, Karmonik C, Via DP, Morrisett JD. Quantitation and localization of

matrix metalloproteinases and their inhibitors in human carotid endarterectomy tissues. *Arterioscler Thromb Vasc Biol*. 2006;26:2351–2358.
18. Sukhova GK, Schonbeck U, Rabkin E, Schoen FJ, Poole AR, Billinghurst RC, Libby P. Evidence for increased collagenolysis by interstitial collagenases-1 and -3 in vulnerable human atheromatous plaques. *Circulation*. 1999;99:2503–2509.
19. Loftus IM, Naylor AR, Goodall S, Crowther M, Jones L, Bell PR, Thompson MM. Increased matrix metalloproteinase-9 activity in unstable carotid plaques. A potential role in acute plaque disruption. *Stroke*. 2000;31:40–47.
20. Schafers M, Riemann B, Kopka K, Breyholz HJ, Wagner S, Schafers KP, Law MP, Schober O, Levkau B. Scintigraphic imaging of matrix metalloproteinase activity in the arterial wall in vivo. *Circulation*. 2004;109:2554–2559.
21. Galis ZS, Sukhova GK, Libby P. Microscopic localization of active proteases by in situ zymography: detection of matrix metalloproteinase activity in vascular tissue. *Faseb J*. 1995;9:974–980.
22. Galis ZS, Khatri JJ. Matrix metalloproteinases in vascular remodeling and atherogenesis: the good, the bad, and the ugly. *Circ Res*. 2002;90:251–262.
23. Nikkari ST, O'Brien KD, Ferguson M, Hatsukami T, Welgus HG, Alpers CE, Clowes AW. Interstitial collagenase (MMP-1) expression in human carotid atherosclerosis. *Circulation*. 1995;92:1393–1398.
24. Halpert I, Sires UI, Roby JD, Potter-Perigo S, Wight TN, Shapiro SD, Welgus HG, Wickline SA, Parks WC. Matrilysin is expressed by lipid-laden macrophages at sites of potential rupture in atherosclerotic lesions and localizes to areas of versican deposition, a proteoglycan substrate for the enzyme. *Proc Natl Acad Sci U S A*. 1996;93:9748–9753.
25. Lee RT, Schoen FJ, Loree HM, Lark MW, Libby P. Circumferential stress and matrix metalloproteinase 1 in human coronary atherosclerosis. Implications for plaque rupture. *Arterioscler Thromb Vasc Biol*. 1996;16:1070–1073.
26. Dollery CM, Owen CA, Sukhova GK, Krettek A, Shapiro SD, Libby P. Neutrophil elastase in human atherosclerotic plaques: production by macrophages. *Circulation*. 2003;107:2829–2836.
27. Brown DL, Hibbs MS, Kearney M, Loushin C, Isner JM. Identification of 92-kD gelatinase in human coronary atherosclerotic lesions. Association of active enzyme synthesis with unstable angina. *Circulation*. 1995;91:2125–2131.
28. Virmani R, Kolodgie FD, Burke AP, Farb A, Schwartz SM. Lessons from sudden coronary death: a comprehensive morphological classification scheme for atherosclerotic lesions. *Arterioscler Thromb Vasc Biol*. 2000;20:1262–1275.
29. Takaya N, Yuan C, Chu B, Saam T, Polissar NL, Jarvik GP, Isaac C, McDonough J, Natiello C, Small R, Ferguson MS, Hatsukami TS. Presence of intraplaque hemorrhage stimulates progression of carotid atherosclerotic plaques: a high-resolution magnetic resonance imaging study. *Circulation*. 2005;111:2768–2775.
30. de Smet BJ, de Kleijn D, Hanemaaijer R, Verheijen JH, Robertus L, van Der Helm YJ, Borst C, Post MJ. Metalloproteinase inhibition reduces constrictive arterial remodeling after balloon angioplasty: a study in the atherosclerotic Yucatan micropig. *Circulation*. 2000;101:2962–2967.
31. Prescott MF, Sawyer WK, Von Linden-Reed J, Jeune M, Chou M, Caplan SL, Jeng AY. Effect of matrix metalloproteinase inhibition on progression of atherosclerosis and aneurysm in LDL receptor-deficient mice overexpressing MMP-3, MMP-12, and MMP-13 and on restenosis in rats after balloon injury. *Ann N Y Acad Sci*. 1999;878:179–190.